THE FASEB JOURNAL • RESEARCH • www.fasebj.org

Ectopic brown adipose tissue formation within skeletal muscle after brown adipose progenitor cell transplant augments energy expenditure

Yang Liu,[*,†] Wenyan Fu,[*,†] Kendall Seese,[†] Amelia Yin,[*,†] and Hang Yin[*,†,1]
[*]Center for Molecular Medicine and [†]Department of Biochemistry and Molecular Biology, University of Georgia, Athens, Georgia, USA

ABSTRACT: Brown adipose tissue (BAT) thermogenesis increases energy expenditure (EE). Expanding the volume of active BAT *via* transplantation holds promise as a therapeutic strategy for morbid obesity and diabetes. Brown adipose progenitor cells (BAPCs) can be isolated and expanded to generate autologous brown adipocyte implants. However, the transplantation of brown adipocytes is currently impeded by poor efficiency of BAT tissue formation *in vivo* and undesirably short engraftment time. In this study, we demonstrated that transplanting BAPCs into limb skeletal muscles consistently led to the ectopic formation of uncoupling protein 1 (UCP1)$^{+pos}$ adipose tissue with long-term engraftment (>4 mo). Combining VEGF with the BAPC transplant further improved BAT formation in muscle. Ectopic engraftment of BAPC-derived BAT in skeletal muscle augmented the EE of recipient mice. Although UCP1 expression declined in long-term BAT grafts, this deterioration can be reversed by swimming exercise because of sympathetic activation. This study suggests that intramuscular transplantation of BAPCs represents a promising approach to deriving functional BAT engraftment, which may be applied to therapeutic BAT transplantation and tissue engineering.—Liu, Y., Fu, W., Seese, K., Yin, A., Yin, H. Ectopic brown adipose tissue formation within skeletal muscle after brown adipose progenitor cell transplant augments energy expenditure. FASEB J. 33, 000–000 (2019). www.fasebj.org

KEY WORDS: engraftment · thermogenesis · UCP1 · obesity · diabetes

Overeating, sedentary lifestyles, and the resulting positive energy balance are the causes of the current epidemics of obesity, type 2 diabetes, and cardiovascular diseases. In mammals, brown adipose tissue (BAT) specializes in nonshivering thermogenesis under cold exposure (1). In response to cold-induced sympathetic activation, BAT elicits uncoupling protein 1 (UCP1)–mediated uncoupled respiration in mitochondria, which transforms caloric energy into heat (1). As such, BAT thermogenesis increases energy expenditure (EE) and lowers food efficiency, and hence holds promise to correct the positive energy balance. Compelling evidence from rodent models indicates that increasing the volume or activity of BAT leads to lean and healthy phenotypes, even with excessive caloric intake (2).

BAT is abundant in small mammals and human infants, in which BAT is critical for protecting vital organs from cold-induced hypothermia. It is now widely accepted that BAT activity is also prevalent in young and lean human adults (3–7). The small number of UCP1^{+pos} adipocytes from adult humans share gene expression signatures with recruitable brown-like adipocytes (also known as beige or brite adipocytes) within white adipose tissues (WATs) in rodents (8, 9). In healthy human adults, the activation of BAT increases EE, posttransplantation sensitivity; beneficial effects supporting the premise that BAT can be therapeutically targeted for human obesity and diabetes (2). However, it is worth noting that BAT activity is low in humans who are obese, diabetic, and aged, who are more likely to be potential patients for BAT-based therapies (3). In addition, BAT in people who are obese, when subjected to the same activating conditions, has a blunted or even no thermogenic response (10, 11). Thus, transplantation of BAT that is responsive to activation represents a promising therapeutic approach for obese and type 2 diabetes.

ABBREVIATIONS: 3D, 3-dimensional; BAPC, brown adipose progenitor cell; BAT, brown adipose tissue; Cidea, cell death–inducing DNA fragmentation factor α-like effector A; dpt, days posttransplantation; EE, energy expenditure; Elovl3, elongation of very long chain fatty acids protein 3; Fabp4, fatty acid binding protein 4; Fasn, fatty acid synthase; FBS, fetal bovine serum; FCCP, carbonyl cyanide p-trifluoromethoxyphenylhydrazone; FNDC5, fibronectin type III domain-containing protein 5; GFP, green fluorescent protein; H&E, hematoxylin and eosin; iBAPC, immortalized BAPC; iBAT, interscapular BAT; IHC, immunohistochemistry; ISO, isoproterenol; OCR, oxygen consumption rate; p-p38, phosphorylated p38; PDGFRα, platelet-derived growth factor receptor α; Pgc1α, peroxisome proliferator-activated receptor γ, coactivator 1α; Pparg2, peroxisome proliferator-activated receptor γ2; qRT-PCR, quantitative RT-PCR; RER, respiratory exchange ratio; SVF, stromal vascular fraction; sWAT, subcutaneous WAT; T3, triiodothyronine; TA, tibialis anterior; UCP1, uncoupling protein 1; WAT, white adipose tissue

[1] Correspondence: University of Georgia, 325 Riverbend Rd., CMM 2228, Athens, GA 30602, USA. E-mail: hyin@uga.edu

doi: 10.1096/fj.201802162RR

Previous studies demonstrated that BAT fat depots from rodents could successfully engraft in epididymal WAT, subcutaneous cavity, the kidney capsule, the anterior chamber of the eye, and skeletal muscles (12–21). The implantation of BAT depots increased EE, glucose tolerance, and insulin sensitivity (18, 20, 21) and protected recipient rodents from obesity, diabetic hyperglycemia, and atherosclerosis (14, 16, 17, 21). Although these proof-of-principle studies substantiated the therapeutic potential of BAT transplantation, such an approach is not readily translatable to clinical therapies because of the scarcity of BAT as a source of transplant. In this regard, adipose progenitor cells represent a reliable cell source for BAT engineering and transplantation. Notably, BAT-resident brown adipose progenitor cells (BAPCs) can efficiently differentiate into brown adipocytes *in vitro* compared with WAT-derived progenitor cells (22). However, the transplant of BAPCs has had limited success so far because of the low cell survival rate and poor BAT formation after BAPC implantation (12). On the other hand, the transplant of BAPC-derived brown adipocytes led to only short-term beneficial effects (see Discussion). Thus, improving the efficiency of BAPC transplantation has substantial clinical implications.

In this study, we examined various BAPC transplantation conditions using immortalized BAPCs (iBAPCS) and immunodeficient mouse models. We discovered that induced BAPCs with increased adipogenic potential (but not *in vitro* differentiated mature brown adipocytes) can form ectopic $UCP1^{+pos}$ adipose tissues within 1 wk after transplantation into uninjured limb muscles in mice. The engraftment efficacy of BAPCs in muscle is better than in the subcutaneous space or subcutaneous WAT (sWAT) depots. We also demonstrated that combining VEGF with iBAPCs during transplantation improved brown adipose–like tissue formation in muscle, which stably engrafted for ≥17 wk after transplantation. The transplantation of iBAPCs resulted in augmented whole-body EE in recipient mice. Intriguingly, although BAT grafts in muscle had decreased UCP1 expression after long-term engraftment, swimming exercise was able to restore UCP1 expression and reverse the whitening *via* sympathetic activation. These findings have implications in future BAT transplantation–based therapies.

MATERIALS AND METHODS

Animals

All animal studies were approved by University of Georgia Institutional Animal Care and Use Committee. Both male and female C57BL/6J (000664) and NOD-SCID (001303) mice (The Jackson Laboratory, Bar Harbor, ME, USA) were used. Animals were housed in a 22°C environment with a 12-h light/dark cycle and given food and water *ad libitum*. NOD-SCID mice were housed in a sterile environment with sterilized food and water.

Adipose tissue stromal vascular fraction isolation

Interscapular BAT (iBAT) was excised from 4-wk-old C57BL/6J mice, minced, and digested with collagenase (Worthington Biochemical Corporation, Lakewood, NJ, USA) in stromal vascular fraction (SVF) isolation buffer (123 mM NaCl, 5 mM KCl, 1.3 mM $CaCl_2$, 5 mM glucose, 100 mM HEPES, and 4% bovine serum albumin) at 37°C. The digestions were filtered through 100-μm filters and centrifuged at 800 *g*. Cell pellets were washed and suspended in SVF culture medium [DMEM containing 20% fetal bovine serum (FBS) and 1% penicillin-streptomycin].

Cell culture and adipogenic differentiation

All cell cultures were maintained at 37°C with 5% CO_2. Cells in SVFs were expanded in SVF culture medium in collagen-coated cell culture dishes and subcultured at ~60% confluence with 0.05% trypsin. SVFs were induced to brown adipogenic lineage with induction medium [DMEM, 10% FBS, 0.5 mM isobutylmethylxanthine, 125 mM indomethacin, 2 mg/ml dexamethasone, 850 nM insulin, 1 nM triiodothyronine (T3), 0.5 mM rosiglitazone, and 1% penicillin-streptomycin] for 2 d. To generate induced BAPCs with increased adipogenic potential, BAPCs were incubated in the induction medium for only 1 d. To differentiate BAPCs into brown adipocytes, BAPCs with a 2-d induction were cultured in differentiation medium (DMEM, 10% FBS, 850 nM insulin, 1 nM T3, 0.5 mM rosiglitazone, and 1% penicillin-streptomycin) for 7 d. To activate β-adrenergic signaling, 10 μM isoproterenol (ISO; MilliporeSigma, Burlington, MA, USA) was added to mature adipocyte cultures for 2 and 6 h. 3T3-L1 cells [American Type Culture Collection (ATCC), Manassas, VA, USA] were cultured following the protocol provided by the ATCC and differentiated following the same adipogenic differentiation protocol as described above for SVFs.

Lentivirus packaging and infection

To immortalize BAPCs, TERT was overexpressed in BAPCs by lentivirus infection. Briefly, pLenti-hTERT (Applied Biological Materials, Vancouver, BC, Canada) and pCMV-eGFP (System Biosciences, Palo Alto, CA, USA) were transfected into 293T cells by polyethylenimine. After 48 h of transfection, 293T culture medium (DMEM containing 10% FBS and 1% penicillin-streptomycin) was collected, filtered with 0.45-μm filters, and incubated with 10% Speedy Lentivirus Concentrator (Applied Biological Materials) at 4°C followed by centrifugation at 4250 *g* for 30 min at 4°C. Pelleted lentivirus particles were resuspended in cell culture medium with 8 μg/ml polybrene (Santa Cruz Biotechnology, Dallas, TX, USA) and incubated with cells for 12 h. After 36–48 h of infection, cells expressing genes of interest were detected and selected by 2 μg/ml puromycin or a green fluorescent protein (GFP) signal.

Seahorse assay

Brown adipose SVFs or 3T3-L1 preadipocytes were plated and differentiated on Seahorse XFe^{24} microplates (Agilent Technologies, Santa Clara, CA, USA) under the conditions previously described. Before Seahorse assays, culture medium were changed to Seahorse XF base medium supplemented with 2 mM glutamine, 1 mM sodium pyruvate, and 4.5 g/L glucose (Agilent Technologies). Cells were placed in a non-CO_2 incubator 1 h prior to Seahorse assay. Oxygen consumption rates (OCRs) were measured *via* the mitochondrial stress test assay with a Seahorse XFe^{24} analyzer following the manufacturer's protocol (Agilent Technologies). To test the response of iBAPC-derived adipocytes to ISO, Seahorse medium with or without ISO (final concentration 10 μM) were injected by the analyzer after measuring the basal respiration. Data were processed *via* Wave software (Agilent Technologies).

Transplantation procedure

All cells for transplantation were washed with PBS on plates, scraped from plates, pelleted by centrifugation, resuspended in

DMEM (4.5 g/L glucose) with or without recombinant VEGFA (200 ng/ml; Thermo Fisher Scientific, Waltham, MA, USA), and loaded into insulin syringes. NOD-SCID mice (8–12 wk old) were used as recipients of transplantation and received ketoprofen (1 mg/kg i.p.) before transplantation. Hair covering the transplantation sites (flank regions and hind limbs) was clipped, and the skin was exposed and sterilized. For transplantation into subcutaneous white fat depots, a small incision was made on the flank skin to expose the subcutaneous fat depot. For transplantation into skeletal muscle, cells were injected either into tibialis anterior (TA) muscle or at 10 sites of various muscles in the upper and lower limbs. After transplantation, all mice received rosiglitazone (10 mg/kg/d; i.p. injection) for 5 consecutive days.

Immunofluorescence imaging

For oil droplet staining, cells were incubated with HCS LipidTOX (Deep Red Neutral Lipid Stain; Thermo Fisher Scientific) and Hoechst 33342 in culture medium for 30 min at 37°C with 5% CO_2 followed by washing with PBS 3 times. For GFP fluorescence imaging in whole-mount tissues, small pieces of iBAPC grafts were excised, briefly washed in PBS, mounted on glass slides, and imaged under an Evos FL fluorescence microscope (Thermo Fisher Scientific). For CD31 immunostaining, cryosections of muscle with BAT grafts were incubated with anti-mouse CD31 antibody (12-0311-81; Thermo Fisher Scientific) at 4°C overnight. Images were captured under an Evos FL fluorescence microscope.

H&E staining and immunohistochemistry staining

Tissues with BAT grafts were excised from mice and fixed in 10% formalin, dehydrated, and embedded in paraffin. For hematoxylin and eosin (H&E) staining, tissue slices (5 μm) were stained with H&E Y. For immunohistochemistry (IHC) staining, paraffin sections were treated with antigen-unmasking buffer (10 mM Tris, 1 mM EDTA, 0.05% Tween 20, pH 9.0) in 93°C for 15 min. Sections were blocked with blocking solution (10% normal goat serum and 1% bovine serum albumin) for 1 h at room temperature and incubated with primary antibodies overnight at 4°C. Anti-UCP1 (ab10983; Abcam, Cambridge, United Kingdom), anti–platelet-derived growth factor receptor α (PDGFRα) (sc-338; Santa Cruz Biotechnology), and anti–Perilipin A (4854; Vala Sciences, San Diego, CA, USA) antibodies were used following the manufacturers' suggested dilution ratios. The endogenous peroxidase was quenched with 3% hydrogen peroxide. Sections were then incubated with secondary antibody for 1 h at room temperature. Slides were developed with diaminobenzidine (Vector Laboratories, Burlingame, CA, USA) for 5 min, followed by hematoxylin counterstaining for 1 min. Images are captured using a Leica 4000B microscope equipped with a Leica DFC420 camera (Leica Microsystems, Wetzlar, Germany).

RNA isolation and quantitative RT-PCR analysis

Total RNA was isolated from tissue, grafts, or cell culture using Trizol reagent (Thermo Fisher Scientific). Total RNA (500 ng) was reverse-transcribed into cDNA (Thermo Fisher Scientific). Diluted cDNA was used in quantitative RT-PCR (qRT-PCR) reactions (SsoAdvanced Universal SYBR Green mix; Bio-Rad, Hercules, CA, USA) on a Bio-Rad CFX384 Real-Time PCR Detection System. C_t values were determined, and expression values were calculated by Bio-Rad CFX Manager Software. Relative expression values were normalized to inner reference genes ribosomal protein S18 and TATA-box binding protein unless stated otherwise. The sequences of qRT-PCR primers used in this study are freely available online (*https://docs.google.com/spreadsheets/d/13LV6Ar9wPP7hN6nKfWTg7yO22xKrFfNMc9jF5Dh5ZH4/edit?usp=sharing*).

Genomic DNA qPCR analysis

Genomic DNA was isolated by phenol:chloroform:isoamyl alcohol (25:24:1) (Thermo Fisher Scientific) extraction with RNase digestion. Diluted genomic DNA was used in qPCR reactions on a Bio-Rad CFX384 Real-Time PCR Detection System. Relative expression values were normalized to inner reference gene Globin. The sequences of genomic qPCR primers used in this study are freely available online *(https://docs.google.com/spreadsheets/d/13LV6Ar9wPP7hN6nKfWTg7yO22xKrFfNMc9jF5Dh5ZH4/edit?usp=sharing)*.

Indirect calorimetry

V_{O_2} and V_{CO_2} were measured using an indirect calorimetry system (Oxymax; Columbus Instruments, Columbus, OH, USA) installed under a constant environmental temperature (22°C) and a 12-h light/dark cycle. Mice in metabolic chambers had free access to food and water. V_{O_2} and V_{CO_2} were normalized to the recorded weekly body weight of each mouse. Total EE was estimated using the equation EE = (kcal/min = $3.81 \times V_{O_2}$) + $1.232 \times V_{CO_2}$.

Mouse swimming exercise

The endurance exercise was carried out as described by Boström *et al.* (24). Briefly, mice swam in a ramp protocol starting at 10 min and swimming twice per day, with a 10-min increase every day until reaching 60 min 2×/d. Mice were swimming in 32–38°C warm water. The swimming procedure lasted for 7 d. To block the β-adrenergic activation, β-adrenergic antagonist propranolol (20 mg/kg) was injected intraperitoneally at 30 min before the start of each bout of swimming exercise.

Western blot

Whole-cell and isolated mitochondrial lysates were prepared by homogenization in RIPA buffer supplemented with proteinase inhibitor cocktail (Thermo Fisher Scientific). Protein concentration was quantified by bicinchoninic acid assays. Protein lysates were loaded on 10% SDS-PAGE gels and transferred to PVDF membranes. The membranes were blocked with 5% nonfat milk and Tris-buffered saline with Tween 20 and probed with primary antibodies: anti–α-Tubulin (T6199; MilliporeSigma), anti-UCP1 (ab10983; Abcam), anti-PKA substrates (9624; Cell Signaling Technology, Danvers, MA, USA), anti-p38 MAPK (8690; Cell Signaling Technology), anti–phosphorylated p38 (p-p38) MAPK (4511; Cell Signaling Technology), and anti–pyruvate dehydrogenase (3205; Cell Signaling Technology) at 4°C overnight. After secondary antibody incubation, membranes were treated with ECL reagents and exposed to X-ray films.

Statistical analysis

All values represent means ± SEM with ≥3 biologic replicates. Statistical significance was determined by 2-tailed Student's *t* tests for comparisons between 2 groups after normality tests or 1-way ANOVA with Bonferroni's *post hoc* tests for multiple comparison.

RESULTS

Overexpressing TERT iBAPCs

This study aims to compare engraftment efficiencies of various BAPC transplantation strategies. The comparisons require a large number of BAPCs that have uniform brown

adipogenic potential. SVFs of iBAT (from 5-d postnatal pups) were isolated as sources for BAPCs. However, the majority of *in vitro* cultured BAPCs lost the brown adipogenic differentiation potential after 5 passages (**Fig. 1*A*, *C*, *D***, primary passage 0 *vs.* passage 5), which limited the use of primary BAPCs in a large-scale comparative transplantation study. To address this issue, we generated iBAPCs following a recently published protocol (24). We isolated iBAT SVFs from C57BL/6 mice (4 wk old) and infected primary SVF cells (passage 0) with TERT-expressing lentivirus. Stable clones (>20 clones) were isolated after puromycin resistance selection, limited dilution, and clonal expansion. Several clones had been randomly selected and continuously cultured for >40

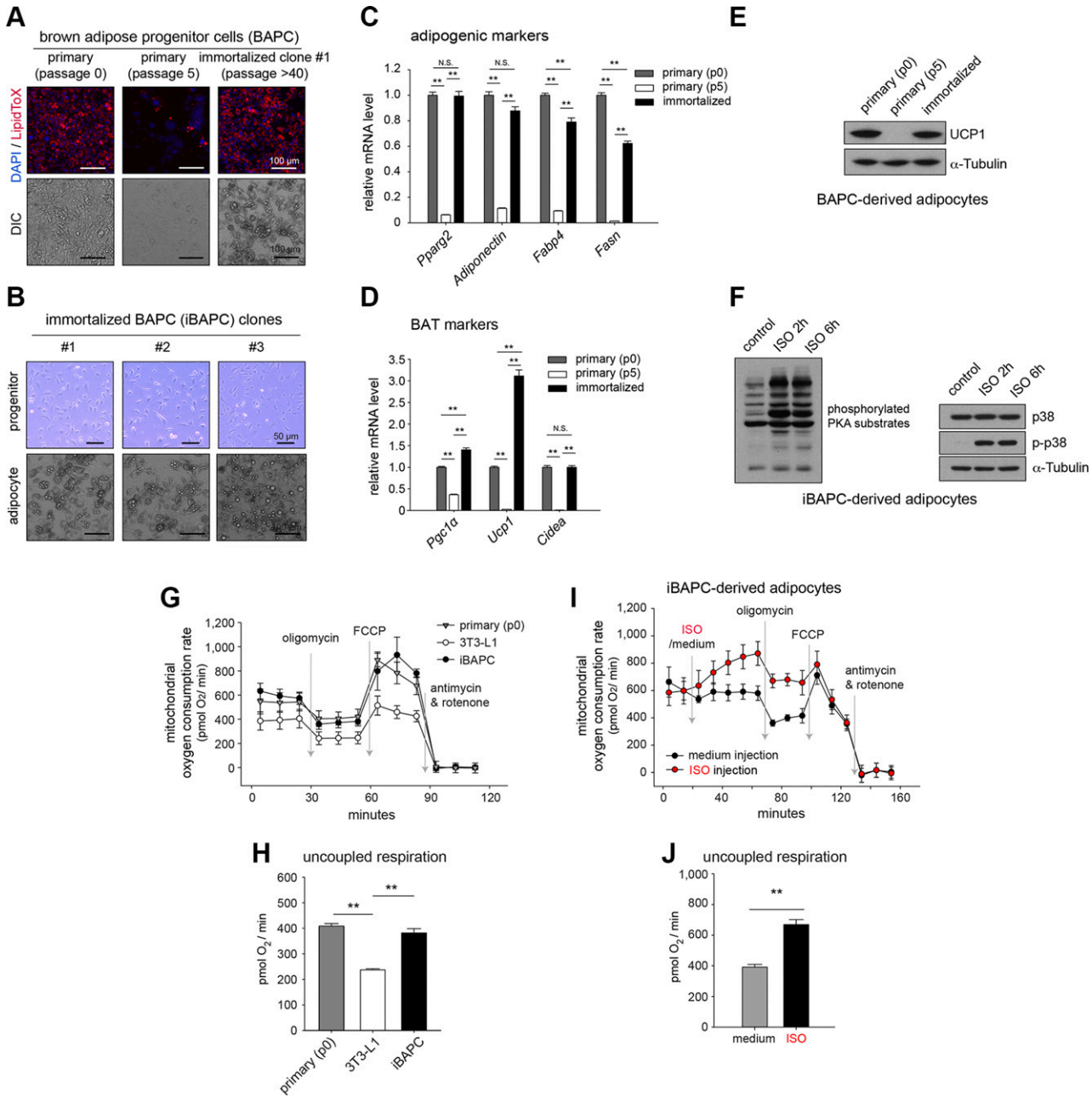

Figure 1. Overexpressing TERT iBAPCs. *A*) Adipocyte cultures derived from primary passage 0 (p0), subcultured passage 5 (p5), and TERT-immortalized brown progenitor cells. Upper: LipidTOX (oil droplets) and DAPI staining. Lower: differential interference contrast (DIC). *B*) The 3 clones of iBAPCs. Upper: iBAPC clones in expansion cultures. Lower: after adipogenic differentiation. *C*) qRT-PCR of adipogenic differentiation markers in adipocytes derived from primary, subcultured, and iBAPCs. *D*) qRT-PCR analysis of BAT lineage markers of the above adipocyte cultures. *E*) UCP1 IBs of the above adipocyte cultures. *F*) Phosphorylated PKA substrates and p-p38 IBs of iBAPC-derived adipocytes treated with ISO. *G*) Seahorse assays showing OCRs of differentiated 3T3-L1 adipocytes, primary brown adipocytes (p0), and iBAPC adipocytes. *H*) Calculated uncoupled respiration rates in the above Seahorse assay. *I*) Seahorse assays showing OCRs of iBAPC adipocytes after acute treatment with 10 μM ISO or medium control. *J*) Calculated uncoupled respiration rates in above Seahorse assay. FCCP, carbonyl cyanide p-trifluoromethoxy-phenylhydrazone; IB, immunoblotting; N.S., not significant. $^{**}P < 0.01$.

passages and retained the adipogenic potential (Fig. 1*B*). iBAPCs had similar adipogenic differentiation potential compared with primary iBAT SVF cells (passage 0), as evidenced by: *1*) the uniform morphology of adipocytes after differentiation (Fig. 1*B*), *2*) the presence of LipidTox^{+pos} oil droplets of 5–10 μm in all adipocytes (Fig. 1*A*; clone 1), and *3*) the largely comparable expression levels of adipocyte markers [peroxisome proliferator-activated receptor γ2 (*Pparg2*), adiponectin (*Adipoq*), fatty acid binding protein 4 (*Fabp4*), and fatty acid synthase (*Fasn*); Fig. 1*C*].

Compared with primary brown adipocytes, the adipocytes differentiated from iBAPCs also expressed comparable (or increased) levels of BAT markers [peroxisome proliferator-activated receptor γ, coactivator 1α (*Pgc1α*), *Ucp1*, and cell death–inducing DNA fragmentation factor α-like effector A (*Cidea*); Fig. 1*D*] and UCP1 protein (Fig. 1*E*). In response to β-adrenergic receptor activation, brown adipocytes have increased activity of PKA, which phosphorylates many downstream targets, including p38 MAPK (2). iBAPC-derived adipocytes treated with ISO (10 μM) for 2 and 6 h had overtly increased phosphorylation of PKA substrates and p-p38 MAPK (Fig. 1*F*), indicating that iBAPC-derived brown adipocytes can be activated *via* the adrenergic receptor pathway. Seahorse assays were performed to measure cellular respiration rates of adipocytes differentiated from 3T3-L1 preadipocytes, primary iBAT SVF cells (passage 0), and iBAPCs. Compared with 3T3-L1–derived adipocytes, primary brown adipocytes and iBAPC-derived adipocytes had elevated levels of basal and uncoupled respiration (Fig. 1*G, H*), which is consistent with active thermogenesis in these adipocytes. The adipocytes differentiated from 3T3-L1 preadipocytes also had a considerable amount of uncoupled respiration, which is consistent with previous reports (26, 27). iBAPC-derived adipocytes had comparable basal and uncoupled respiration to primary brown adipocytes, indicating that immortalization and extensive *in vitro* culture had no adverse effect on the thermogenic capacity of iBAPC-derived adipocytes (Fig. 1*G, H*). In addition, iBAPC-derived adipocytes had elevated uncoupled respiration upon acute ISO treatment (Fig. 1*I, J*), which further confirmed their response to β-adrenergic activation.

Induced iBAPCs developed into adipose tissue in limb muscles but not in subcutaneous space or sWAT depots

The successful engraftment of brown fat depots and white preadipocytes at subcutaneous locations has been reported before (27). It has also been reported that the transplantation of bone morphogenetic protein 7–treated stem cells antigen-1^{+pos} multilineage progenitor cells developed into BAT in limb skeletal muscle but not in subcutaneous locations (28). We sought to compare the engraftment efficiency of iBAPCs transplanted at subcutaneous spaces, subcutaneous white fat depots, and limb muscles. To ease the identification of engrafted cells, GFP^{+pos} iBAPCs were made by lentiviral transduction. To increase the adipogenic potential, iBAPCs were cultured to reach full confluence for 24 h and further incubated with brown adipogenic induction medium for another 24 h (hereafter called induced iBAPCs). A total of 2×10^6 induced iBAPCs were injected into the subcutaneous space at the flank region, a subcutaneous inguinal white fat depot (sWAT), or Tibialis anterior (TA) muscle in the lower hind limb of immunodeficient NOD-SCID mice. At 1 wk after transplantation [7 d posttransplantation (dpt)], grafts were found at the local injection sites within the subcutaneous space and sWAT depots, whereas intramuscular transplanted cells were found dispersed along longitudinal axes of the transplanted TA muscles (**Fig. 2*A***). Whole-mounted skin, sWAT, and TA muscles with iBAPC grafts were checked under a fluorescence microscope for the morphology of GFP^{+pos} engrafted cells at 7 dpt (Fig. 2*B*). Most GFP^{+pos} engrafted cells in subcutaneous locations or in sWAT depots retained preadipocyte-like irregular morphology, whereas most GFP^{+pos} cells engrafted in TA muscles resembled adipocytes. The iBAPC grafts were also examined by IHC for GFP, PDGFRα (a preadipocyte marker), and Perilipin A (a mature adipocyte marker). The majority of engrafted cells in TA muscles were Perilipin^{+pos} and PDGFRα^{-}, whereas most engrafted cells at subcutaneous space and within sWAT were PDGFRα^{+pos} and Perilipin^{-neg} (Fig. 2*C*), suggesting the poor differentiation of iBAPCs at these places. In addition, iBAPC grafts isolated from TA muscles had overtly higher expression levels of adipocyte markers (*Pparg2*, *Adipoq*, *Fabp4*, and *Fasn*) than grafts isolated from the other 2 locations (Fig. 2*D*). Thus, TA muscle appeared as a superior transplantation site for iBAPCs compared with the subcutaneous space and sWAT.

Induced iBAPCs had higher engraftment potential than differentiated iBAPC-derived brown adipocytes in limb skeletal muscles

Next, we compared the engraftment efficiencies of induced iBAPCs *vs. in vitro* differentiated iBAPC-derived mature brown adipocytes after transplantation into limb muscles. A total of 2×10^6 induced iBAPCs or iBAPC-derived mature brown adipocytes were injected into TA muscles. At 7 dpt, induced iBAPC transplantation consistently led to a large number of GFP^{+pos} adipocyte-like cells engrafted in TA muscles, whereas much fewer GFP^{+pos} cells could be found after mature brown adipocyte transplantation (**Fig. 3*A***). To quantify the numbers of remaining GFP^{+pos} grafted cells, genomic DNA was isolated from iBAPC-transplanted TA muscles either right after the transplantation (input) or at 7 dpt; qPCRs for GFP coding sequence (specific to iBAPC graft genome) and the β-globin gene (in genomes of both iBAPCs and host cells) were performed to determine the percentages of remaining iBAPC graft genome copy numbers. qPCR assays revealed that 12.1% of transplanted induced iBAPCs survived at 7 dpt, whereas this rate dropped to 2.7% for mature brown adipocytes (Fig. 3*B*). Moreover, histologic examinations indicated that the remaining cells from mature brown adipocyte transplantation had a mesenchyme-like morphology, which was distinct from the adipose grafts formed after induced iBAPC transplantation (Fig. 3*C*).

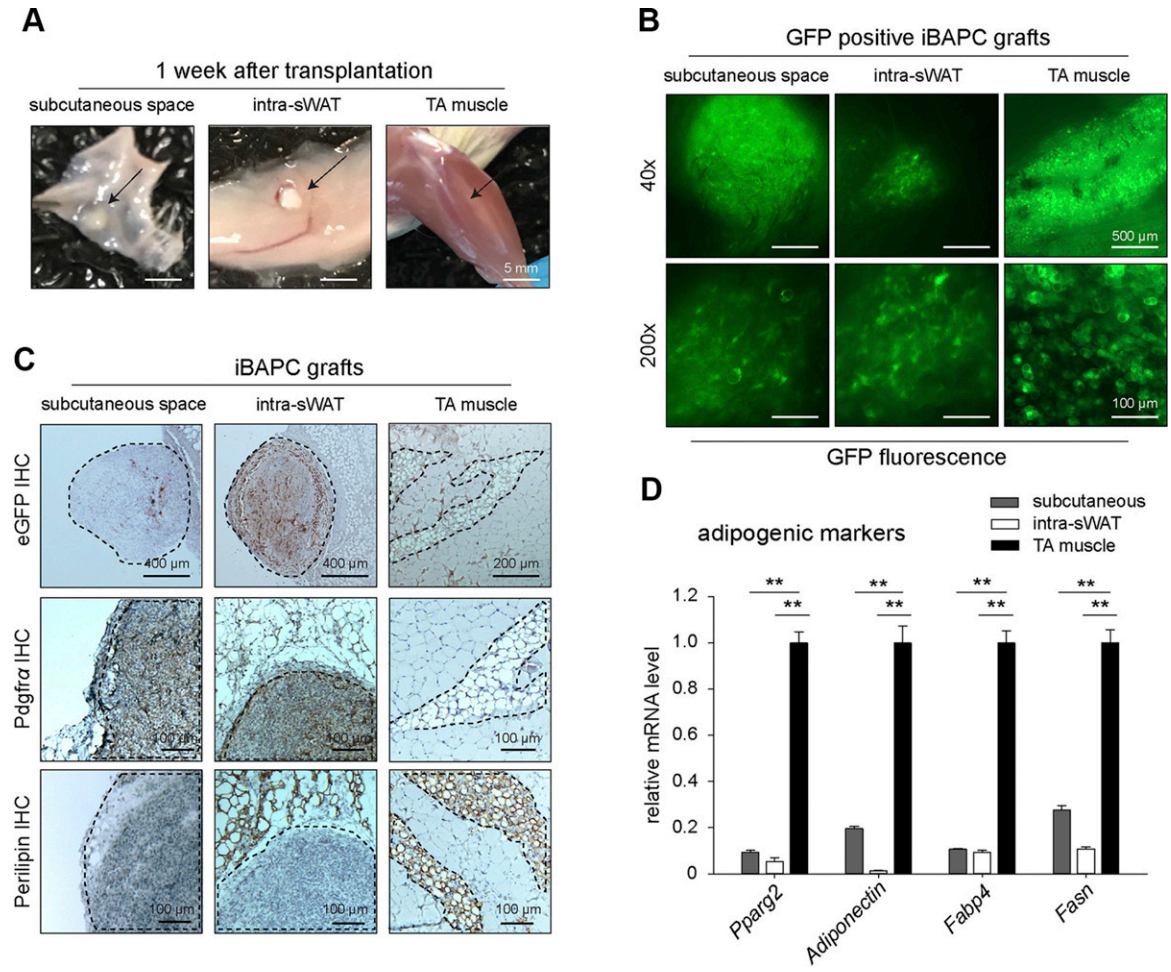

Figure 2. Induced iBAPCs developed into adipose tissues in limb muscles. *A*) Engraftments (arrows) developed within subcutaneous space, sWAT, and TA muscle after iBAPC transplantation (7 dpt). *B*) GFP^{+pos} engrafted cells at the above transplantation sites. *C*) GFP, PDGFRα, and Perilipin IHC of iBAPC grafts. Dotted lines enclose engrafted cells. *D*) qRT-PCR of adipogenic markers in iBAPC grafts ($n = 3$ per transplantation site). eGFP, enhanced GFP. $^{**}P < 0.01$.

qRT-PCR further confirmed that the expression levels of BAT markers [*Ucp1*, *Cidea*, and elongation of very long chain fatty acids protein 3 (*Elovl3*)] were much lower in TA muscles transplanted with mature brown adipocytes than those engrafted with induced iBAPCs (Fig. 3*D*). Therefore, induced iBAPCs had higher engraftment potential than iBAPC-derived mature brown adipocytes after transplanted into limb muscle.

Combining induced iBAPCs with VEGF during transplantation improved brown adipocyte characteristics of intramuscular grafts

VEGF plays a pivotal role in angiogenesis and has been widely applied in tissue transplantation (29). Next, we investigated whether VEGF can improve the engraftment potential of iBAPCs. A total of 2×10^6 induced iBAPCs were mixed with recombinant human VEGF (20 ng) or vehicle (PBS) and separately transplanted into TA muscles. At 7 dpt, TA muscles transplanted with iBAPCs along with VEGF had an elevated mRNA level of endothelial cell marker platelet and endothelial cell adhesion molecule 1 (*Cd31*) than the muscles that were transplanted only with iBAPCs (**Fig. 4*A***). H&E staining and CD31 immunofluorescence staining of TA muscle cross-sections further verified the increase of blood vessels in TA muscles treated with VEGF (Fig. 4*B, C*). qRT-PCR indicated that VEGF did not affect the adipocyte markers (*Pparg2*, *Adipoq*, *Fabp4*, and *Fasn*) in transplanted muscles (Fig. 4*D*). Intriguingly, combining VEGF during transplantation resulted in 15–20-fold higher brown adipocyte markers (*Ucp1*, *Cidea*, and *Elovl3*; Fig. 4*E*) and elevated UCP1 protein expression in iBAPC-derived adipose grafts (Fig. 4*F*). Thus, VEGF appeared to improve brown adipocyte characteristics after intramuscular transplantation of induced iBAPCs. To understand whether VEGF has a cell-autonomous effect on iBAPCs, we treated *in vitro* cultured iBAPCs with VEGF (100 ng/ml) during brown adipogenic differentiation. VEGF did not improve adipogenesis or increase the expression of BAT markers (Fig. 4*G*).

Intramuscular transplantation of induced iBAPCs with VEGF augmented EE

Different iBAPC clones may have variable engraftment potential and propensities to form BAT within muscle. To

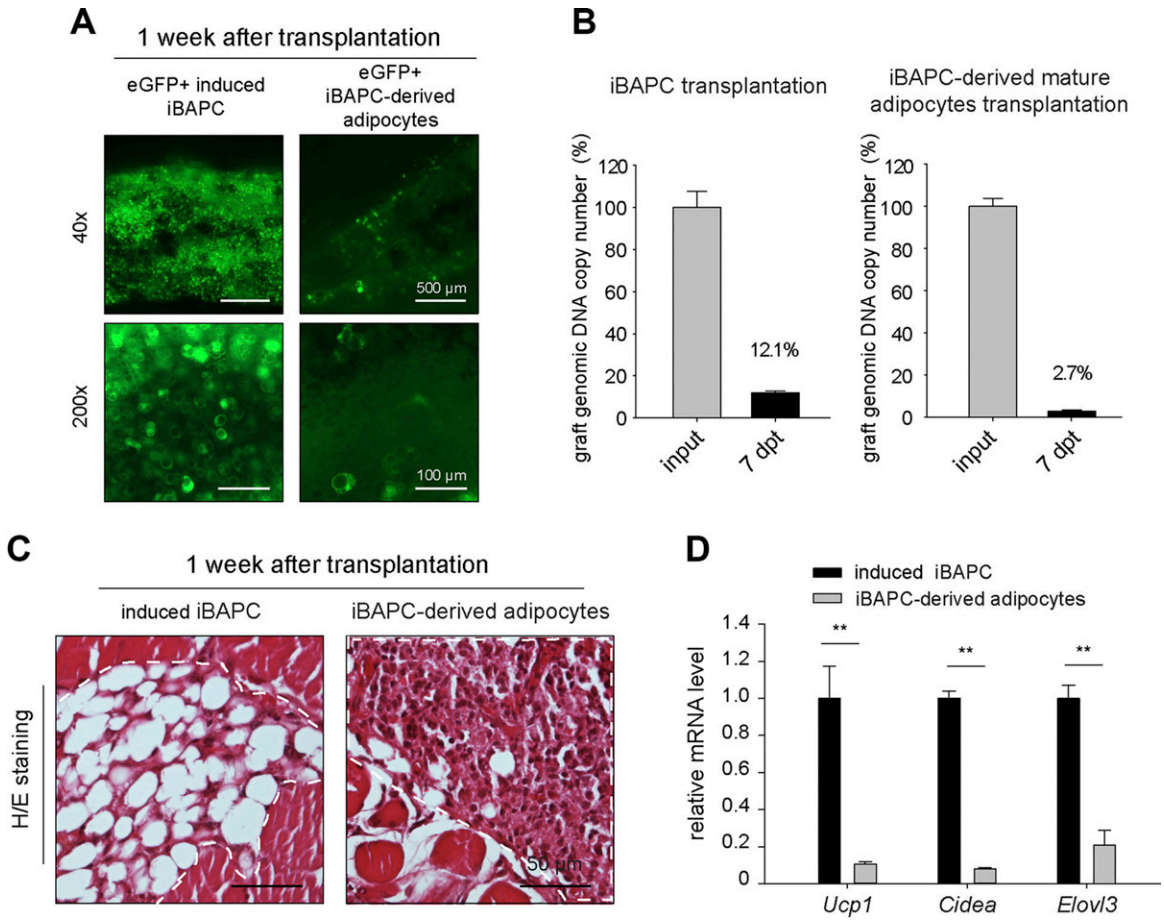

Figure 3. Induced iBAPCs had higher engraftment potential than iBAPC-derived mature adipocytes in limb skeletal muscles. *A*) GFP^{+pos} engrafted cells in TA muscles developed from induced iBAPCs and iBAPC-derived mature adipocytes. *B*) qPCR of genomic DNA copy numbers from GFP^{+pos} grafts remained in TA muscle at 0 (input) and 7 dpt ($n = 3$ per group per time point). *C*) H&E staining of TA muscles transplanted with induced iBAPCs or iBAPC-derived mature adipocytes (7 dpt). Dotted lines enclose engrafted cells. *D*) qRT-PCR of BAT markers in the above transplanted muscles ($n = 3$ per group). eGFP, enhanced GFP. $^{**}P < 0.01$.

investigate the clonal variation of iBAPC, we separately transplanted 3 clones of iBAPCs (clones shown in Fig. 1*B*) with VEGF into TA muscles. At 7 dpt, all 3 clones of the iBAPCs consistently developed into adipose grafts in muscle (**Fig. 5*A***). To verify the BAT characteristics of grafts, we compared *Ucp1* mRNA levels in the iBAPC-derived grafts with *bona fide* BAT, beige fat (sWAT after 3-d 4°C treatment), and white fat (sWAT, at 22°C), as well as with primary brown adipocytes (passage 0). To exclude the contamination from attached muscle tissues in dissected iBAPC grafts, we normalized *Ucp1* mRNA levels to adipocyte markers (*Pparg2, Adipoq*, *Fabp4*, and *Fasn*), which have very low levels in muscle. We found that grafts from 3 iBAPC clones had variable *Ucp1* levels, but 2 out of 3 clones had higher or similar *Ucp*1 levels compared with beige fat (Fig. 5*B*). Notably, although iBAPC grafts had lower *Ucp1* levels than iBAT or primary brown adipocytes, all of the examined grafts had higher *Ucp1* levels than white fat. In addition, UCP1 protein was also readily detectable from mitochondria isolated from TA muscles transplanted with iBAPCs (Fig. 5C). Thus, iBAPC transplantation consistently led to $UCP1^{+pos}$ adipose grafts in limb muscles.

Next, we investigated whether the ectopic engraftment of brown adipocytes in muscle augments the whole-body EE To increase the amount of BAT grafts in muscle, 1×10^7 iBAPCs were mixed with VEGF (100 ng) and transplanted at 10 sites in both upper and lower hindlimb muscles, including TA, gastrocnemius, and rectus femoris muscles, on both sides of hindlimbs. At 7 dpt, adipose grafts can be observed within all muscle groups (Fig. 5*D*). The total amount of intramuscular iBAPC-derived adipose grafts was estimated to be about 200 mg in this large-scale transplantation.

We next performed indirect calorimetry for mice that received large-scale iBAPC transplantation. The mice were individually housed in metabolic chambers and subjected to calorimetry measurements 1 wk before (pretransplantation) and 1 wk after transplantation (posttransplantation). In light cycles, the transplantation of iBAPCs increased EE and V_{O_2} and decreased the respiratory exchange ratio (RER; Fig. 5*E–G*). In contrast, the mock transplantation (VEGF in saline) did not alter the above parameters (Fig. 5*E–G*). In dark cycles, the transplantation of iBAPCs resulted in a better increase of EE and V_{O_2} but did not alter RER (Fig. 5*E, F, H*). For both

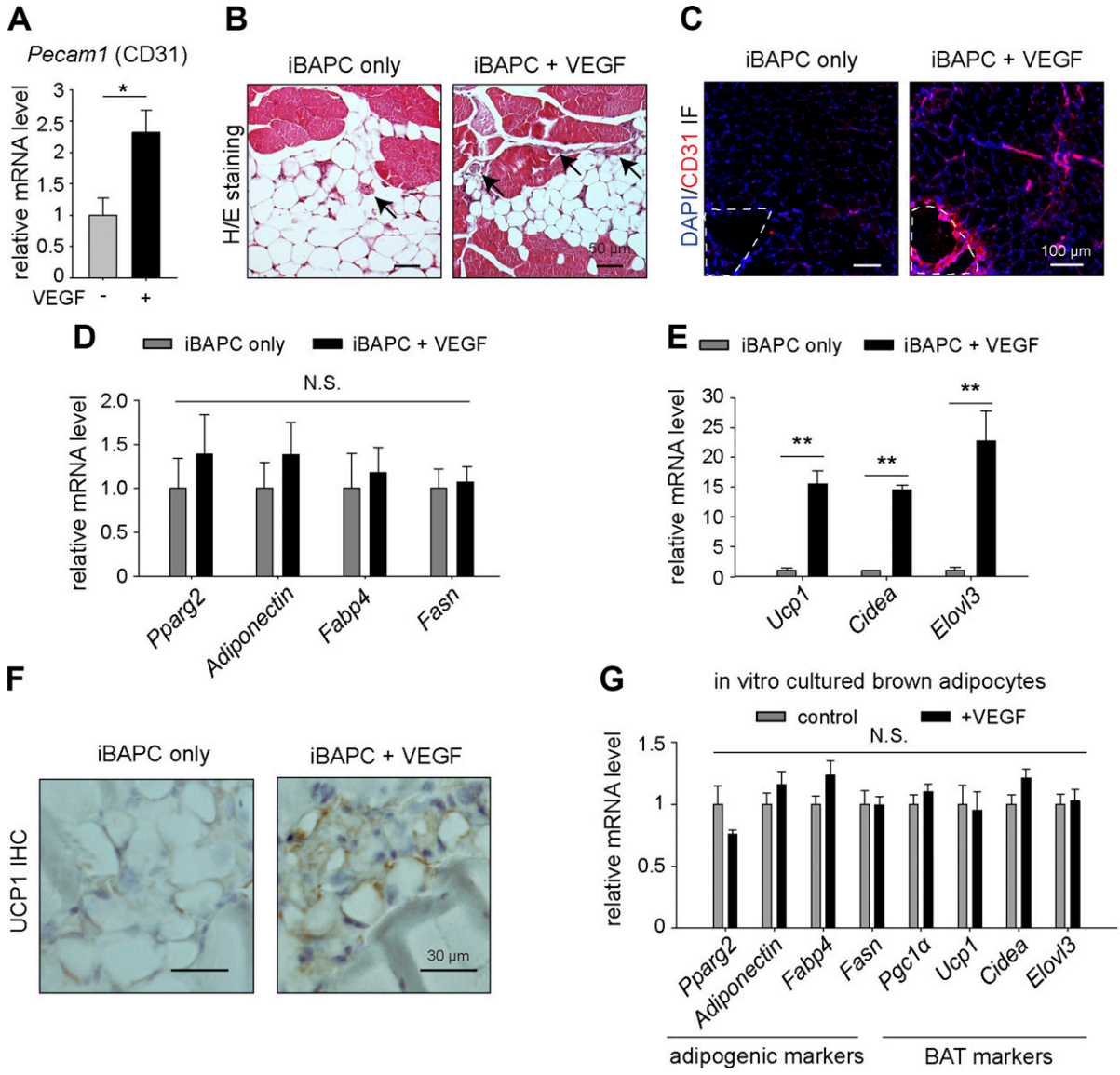

Figure 4. Combined induced iBAPCs with VEGF improved brown adipocyte characteristics of intramuscular adipose grafts. *A*) qRT-PCR of *Pecam1* in TA muscles with or without VEGF during iBAPC transplantation ($n = 3$ per group). *B*) H&E staining showing increased blood vessels (arrows) in TA muscles with VEGF. *C*) CD31 immunofluorescence (IF) showing increased $CD31^{+pos}$ cells in TA muscles with VEGF. *D*) qRT-PCR of adipogenic markers in the above TA muscle samples ($n = 3$ per group). *E*) qRT-PCR of BAT markers ($n = 3$ per group). *F*) UCP1 IHC of adipose grafts in TA muscle with or without VEGF. *G*) qRT-PCR assays of adipocyte markers and BAT markers in *in vitro* cultured iBAPC-derived brown adipocytes treated with or without VEGF ($n = 3$ per group). N.S., not significant; Pecam1, platelet and endothelial cell adhesion molecule 1. $^{**}P < 0.01$.

light and dark cycles, the transplantation of iBAPCs in hind limb muscles did not affect the physical activity of transplanted mice (Fig. 5*G*, *H*). Therefore, intramuscular transplantation of iBAPCs augmented the whole-body EE in recipient mice.

Exercise restored the brown adipocyte characteristics of long-term iBAPC grafts in skeletal muscle

Next, we investigated the long-term engraftment capability of iBAPCs in muscle. After 5 or 15 wk of iBAPC transplantation, adipose grafts could still be consistently observed within TA muscles (**Fig. 6*A***; H&E). However, those long-term adipose grafts (5 and 15 wk) adopted morphologies of WAT and UCP1 IHC confirmed the reduction of UCP1 protein in the long-term grafts compared with 1-wk grafts (Fig. 6*A*). qRT-PCR of transplanted TA muscles further confirmed that long-term grafts (15 wk) had reduced expression levels of *Ucp1* and *Cidea* mRNAs (declined to ~20% of 1-wk grafts; Fig. 6*B*). Interestingly, long-term engraftment did not affect the expression of *Pgc1α* or *Elovl3* in iBAPC grafts (Fig. 6*B*), suggesting some BAT characteristics remained in long-term grafts.

Laboratory mice raised in standard cage conditions are sedentary (30). Exercise (particularly endurance exercise) increases catecholamine levels in the circulation and in skeletal muscles (31) and stimulates the release of thermogenic myokine Irisin (32). Thus, we investigated

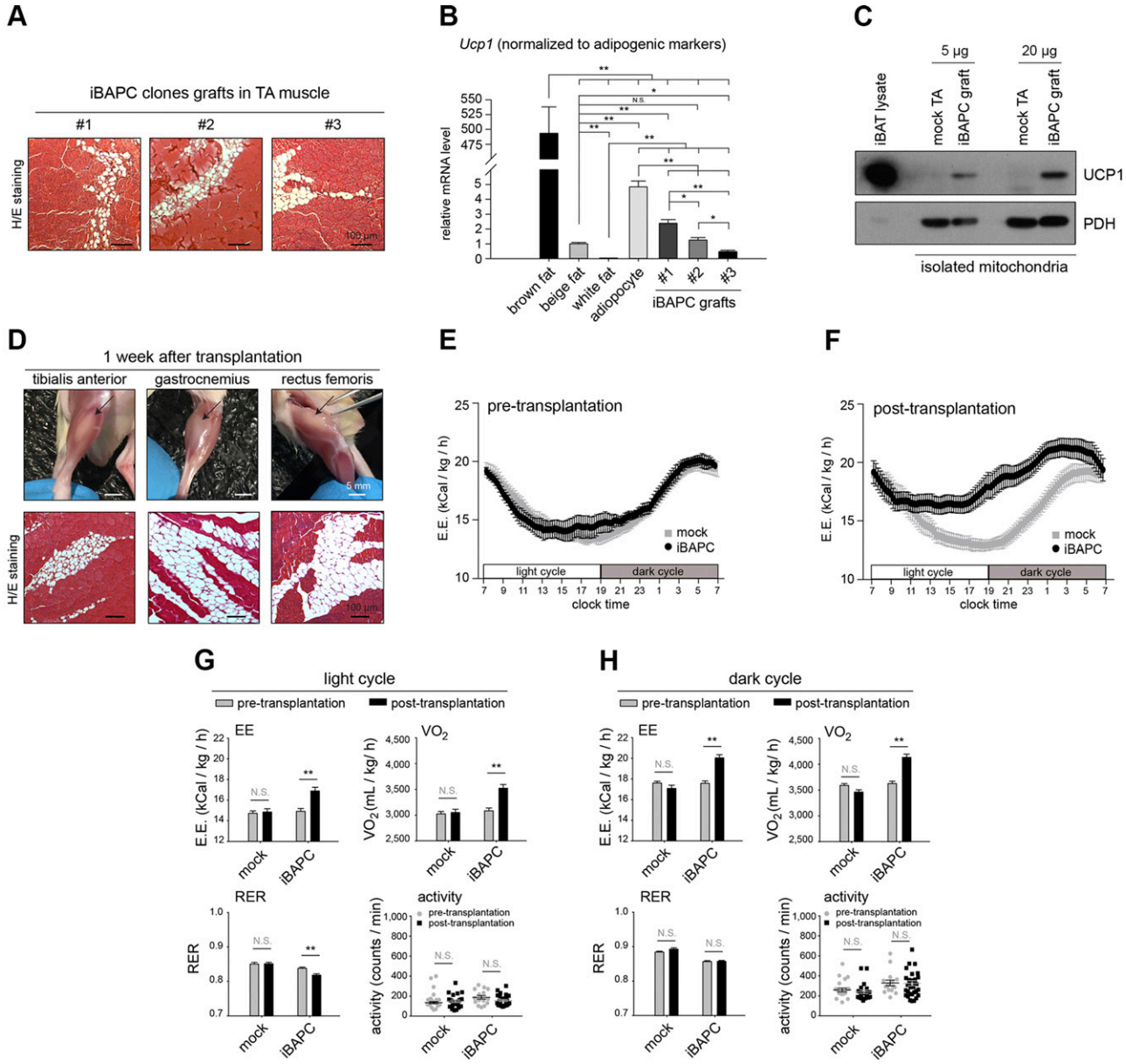

Figure 5. Intramuscular transplantation of iBAPCs augmented EE *A*) H&E staining of adipose grafts in TA muscles transplanted with 3 iBAPC clones (7 dpt). *B*) *Ucp1* qRT-PCR in iBAT, beige fat (sWAT after 3-d exposure to 4°C), white fat (sWAT at 22°C), primary brown adipocytes, and adipose grafts from iBAPC clones ($n = 3$; 7 dpt). The *Ucp1* mRNA levels were normalized to adipogenic markers *Pparg2*, *Adipoq*, *Fabp4*, and *Fasn*. *C)* UCP1 IBs of mitochondria isolated from mock or iBAPC-transplanted TA muscles (clone 1; 7 dpt). Pyruvate dehydrogenase (PDH) served as a loading control for mitochondrial proteins. *D*) Upper: pictures showing adipose grafts (arrows) in TA, gastrocnemius, and rectus femoris. Lower: H&E staining of the above muscles. *E*) EE values in dark and light cycles before transplantation ($n = 4$ per group). *F*) EE values in dark and light cycles after mock and iBAPC transplantation (with VEGF; $n = 4$ per group). *G*) Indirect calorimetry data showing the light cycle values of E.E., VO_2, RER, and activity before and after mock or iBAPC transplantation ($n = 4$ per group). *H*) Indirect calorimetry showing the dark cycle values of EE, VO_2, RER, and activity before and after mock or iBAPC transplantation ($n = 4$ per group). IB, immunoblotting; N.S., not significant. $^*P < 0.05$, $^{**}P < 0.01$.

whether endurance exercise may improve the long-term maintenance of BAT characteristics in iBAPC-derived grafts. After 15 wk of iBAPC transplantation, recipient mice were randomly separated into a nonexercise control group and a swimming exercise group; the latter were subjected to a ramp swimming protocol as previously described by Boström *et al*. (32). After 1 wk of swimming exercise, exercised mice had increased fibronectin type III domain-containing protein 5 (*Fndc5*) mRNA levels (encoding the protein precursor of irisin; 1.4-fold increase) and *Pgc1α* (1.3-fold increase) in engrafted TA muscles compared with the control mice (Fig. 6*C*). Intriguingly, swimming drastically increased *Ucp1* mRNA level (5.3-fold increase) in long-term grafts and normalized its expression to the level of 1-wk grafts (compare with Fig. 6*B*). In addition, *Pgc1α*, *Ucp1*, *Cidea*, and *Elovl3* mRNAs were also increased in sWAT and BAT after swimming (Fig. 6*D*, *E*). UCP1 IHC further confirmed the increase of UCP1

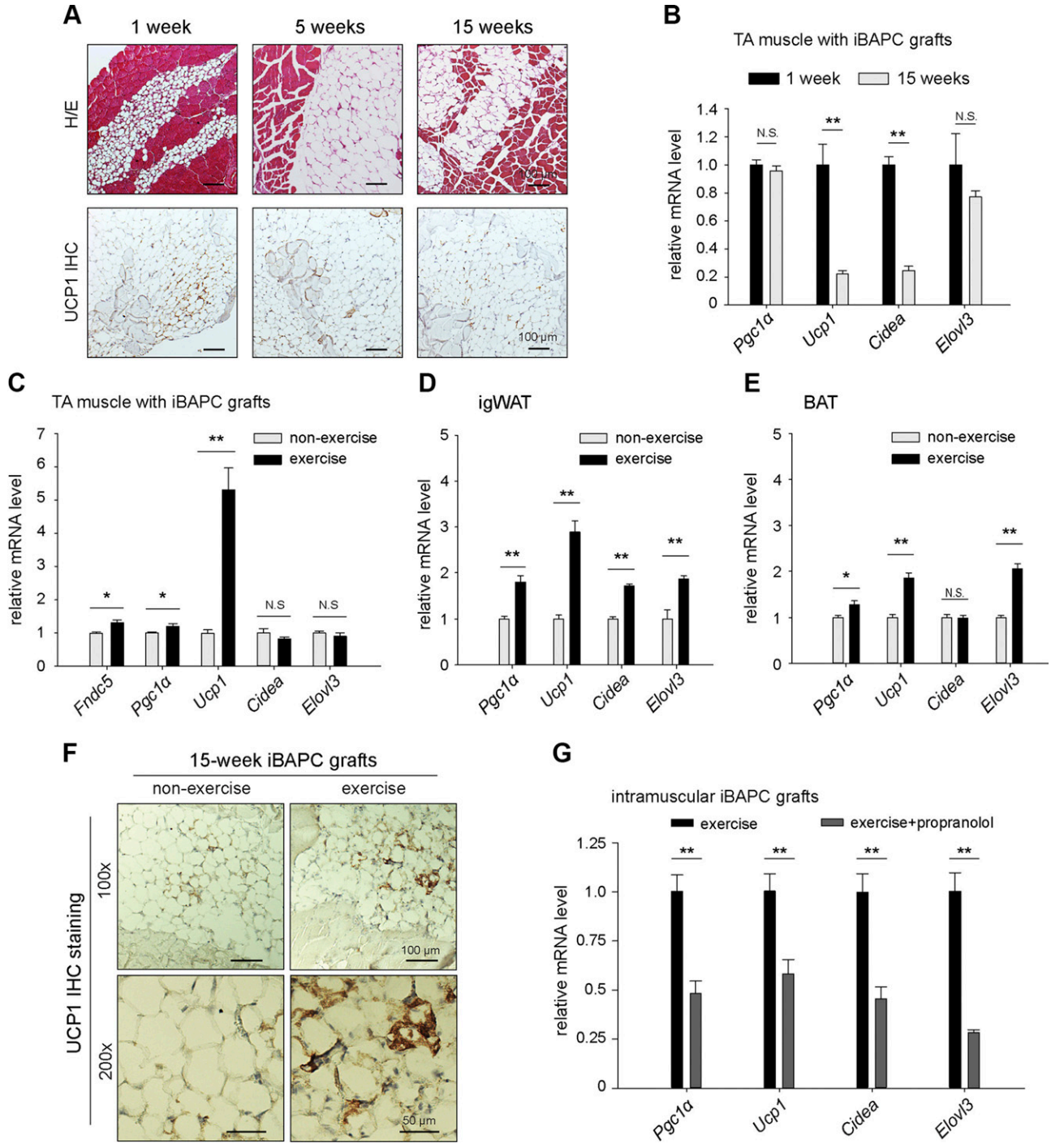

Figure 6. Swimming exercise restored the brown adipocyte characteristics of long-term iBAPC grafts in skeletal muscle. *A*) H&E staining (upper) and UCP1 IHC (lower) of adipose grafts in TA muscles after 1, 5, and 15 wk of iBAPC transplantation. *B*) qRT-PCR of BAT markers in adipose grafts at 1 and 15 wk ($n = 3$ per group). *C*) qRT-PCR of *Fndc5* and BAT markers in engrafted muscles after 1 wk swimming exercise ($n = 3$ per group). *D*) qRT-PCR of BAT markers in sWAT after 1 wk swimming exercise ($n = 3$ per group). *E*) qRT-PCR of BAT markers in iBAT after 1 wk swimming exercise ($n = 3$ per group). *F*) UCP1 IHC showing the increase of UCP1 in iBAPC-derived adipose grafts after swimming exercise. *G*) qRT-PCR showing the reduction of BAT markers in intramuscular iBAPC grafts after swimming exercise with propranolol treatment ($n = 4$ per group). N.S., not significant. $^*P < 0.05$, $^{**}P < 0.01$.

expression in long-term grafts by swimming (Fig. 6*F*). Thus, swimming exercise can reverse the decline of UCP1 in long-term iBAPC grafts in muscle. Next, we investigated whether the above effect is mediated by β-adrenergic activation during swimming. To this end, mice with long-term engraftments were treated propranolol (20 mg/kg; i.p. injection) or vehicle (saline) 30 min before each round of swimming training. Propranolol repressed *Pgc1α, Ucp1, Cidea,* and *Elovl3* levels in iBAPC-derived adipose grafts in swimming-exercised mice (Fig. 6*G*).

Thus, the effects of swimming exercise on iBAPC grafts are, at least partially, mediated by β-adrenergic activation.

DISCUSSION

This study compared various transplantation strategies and demonstrated that the transplantation of induced iBAPCs with VEGF into multiple limb muscles consistently resulted in the formation of UCP1^{+pos} BAT *in vivo* with long-term engraftment capability. Compared with the subcutaneous cavity and sWAT depots, skeletal muscle supported better brown adipogenic differentiation and engraftment. Compared with mature brown adipocytes, induced iBAPCs had better engraftment potential. The intramuscular transplantation of iBAPCs augmented the whole-body EE Although UCP1 expression declined in long-term BAT grafts in muscle, exercise was able to restore UCP1 expression.

Following a recently published protocol (24), we successfully established single-cell clones from immortalized mouse BAPCs by overexpressing TERT. The immortalization of BAPCs allows us to compare various transplantation strategies using a large number of iBAPCs with relatively uniform brown adipogenic differentiation potential. Overexpressing TERT has been reported to successfully immortalize multipotent neural cells and dental pulp progenitor cells without tumorigenic potential (33, 34). In this study, iBAPC transplantation at various sites of NOD-SCID immunocompromised mice did not result in any tumor formation. Although clonal differences exist, *Ucp1* expression in iBAPC-derived adipose grafts are generally comparable with beige fat, supporting the therapeutic potential of this transplantation approach. Because iBAPCs can be clonally selected, easily expanded, and efficiently differentiated into a large amount of UCP1^{+pos} brown adipocytes *in vivo*, perspective generation of immortalized human BAPCs from individual patients may be a feasible strategy to support brown adipocyte–based transplantation therapies. To this end, more stringent characterization of immortalized human BAPCs is warranted in the future.

In this study, induced iBAPCs were paradoxically more prone to engraft and give rise to BAT in skeletal muscle than fully differentiated mature adipocytes. The exact reason for this difference is unknown; however, we postulate that the high metabolism rate of mature brown adipocytes, when transplanted locally in large numbers, may lead to quick exhaustion of nutrients and oxygen in the local transplant site and end in massive cell death. The qPCR quantification of genome copy numbers from grafts supports this notion because only 2.7% of mature adipocytes remained in transplanted TA muscles, whereas 12.1% of induced iBAPCs still remained under the same condition. A recent study indicated that hyaluronic acid–based hydrogels facilitates the survival and engraftment of human WAT–derived multipotent stem cells in the subcutaneous cavity (35). Future studies may further explore innovative 3-dimensional (3D) matrix or transplantation supplements that support the sustained release of nutrients and oxygen in the transplant site before VEGF-induced angiogenesis establishes sufficient perfusion in the implants.

This study revealed that including VEGF in BAPC transplantation enhances the formation of BAT in muscle. Intriguingly, VEGF did not affect the expression of adipogenic markers but up-regulated the expression levels of BAT markers in transplants. Notably, neither adipogenesis nor brown adipocyte markers were affected by VEGF during the *in vitro* differentiation of iBAPCs in this study. This observation is consistent with a previous report that VEGF overexpression did not alter brown adipogenic differentiation of SVFs (36). Given these observations, the beneficial effect of VEGF in iBAPC transplantation is likely a result of its proangiogenic activity in muscle, which echoes the above postulation that increasing vasculature and nutrients and oxygen supplies may improve the survival and engraftment efficiency of iBAPCs. Interestingly, brown adipocytes are known to release VEGF, which promotes the thermogenic capacity and tissue maintenance of BAT (37–39). Future studies on VEGF dosages, treatment duration, and the mechanism of action in iBAPC transplantation may shed light on the optimization of this potential therapeutic strategy.

A readily accessible source of autologous BAPCs and brown adipocytes from individual patients is a prerequisite for brown adipocyte–based transplantation therapies. Several recent studies demonstrated that BAPCs can be isolated and expanded from multiple sources in human adults and generate brown adipocytes with engraftment potential. First, adipose progenitors isolated from microvessels in human subcutaneous adipose tissues were shown to differentiate into UCP1^{+pos} brown-like adipocytes with the adenylate cyclase activator forskolin (40). Transplantation of these cells with matrigel in the subcutaneous cavity led to improved glucose tolerance in NOD-SCID IL2rg^{null} mice. Second, Silva *et al.* (41) reported the successful isolation of human brown adipose–derived stem cells from mediastinal adipose tissue, which are capable of clonal expansion and multilineage differentiation. These cells can differentiate into functional brown adipocytes with the presence of recombinant FNDC5 and, when cultured in 3D scaffolds, can engraft in the subcutaneous cavity for 5 wk. Lee *et al.* (42) showed that human orbital adipose–derived mesenchymal stromal cell differentiated into thermogenic brown adipocytes and elicited a series of benefits in energy, lipid, and glucose metabolism after continuous administration (every 2 wk) in the abdominal cavity of diet-induced obese mice. Besides adipose tissues, BAPCs have also been shown to exist in human and mouse skeletal muscles (28, 43). Also, brown adipocytes for autologous transplantation can be derived from human induced pluripotent cells (44–46). The transplants of these induced pluripotent stem cell–derived brown adipocytes repressed obesity and diabetes within 2–4 wk posttransplantation. Notably, all of the above studies involved the transplantation of differentiated mature brown adipocytes without the use of VEGF and, inevitably, attained only short-term engraftment. Thus, the transplantation strategies implicated in the present study would be instructive for future human BAPC-related transplantation.

This study revealed that skeletal muscle is an excellent transplantation site for BAPC transplantation and *de novo* BAT formation *in vivo*. This is conceivably due to many similarities between BAT and skeletal muscles. First, like BAT, skeletal muscle tissue contains a plethora of blood vessels. A high level of tissue perfusion is both critical for providing ample energy fuel and oxygen in support of thermogenesis and crucial for quickly dissipating heat *via* the bloodstream so as to avoid heat stress in thermogenic tissues. In this sense, skeletal muscle, as a thermogenic tissue capable of shivering thermogenesis, is endowed with this natural advantage to support thermogenesis in BAT grafts. Second, like BAT, skeletal muscle is densely innervated with sympathetic nerves, which releases norepinephrine (47). Norepinephrine is important for acute thermogenic activation of BAT *via* the β-adrenergic receptor-cAMP-PKA signaling pathway (1). In addition, continuous sympathetic inputs are also crucial for the maintenance of thermogenic capacity in both BAT and beige adipocytes (48–50). As the release of norepinephrine in skeletal muscle increases during muscle contraction (particularly during exercise), it is interesting to speculate that physical activity not only activates thermogenesis but also sustains thermogenic capacity in skeletal muscle-embedded BAT grafts. This speculation is in line with our observations that *1*) BAPC transplantation augmented the whole-body EE more evidently during dark cycles, *2*) endurance exercise was capable of reversing the whitening of BAPC grafts in skeletal muscle, and *3*) the restoration of *Ucp1* expression indeed depends on β-adrenergic activation. In line with the findings in this study, obesity-resistant 129S6/SvEvTac mice have ectopic $UCP1^{+pos}$ brown adipocytes interspersed between muscle bundles, whereas obesity-prone C57BL/6 mice have few such brown adipocytes in the muscle (51). In addition, the induction of ectopic brown adipocytes (from muscle stem cell differentiation) in muscle also augmented EE and protects the mice from diet-induced obesity (52). Thus, compared with many other tissues and locations, skeletal muscle may provide excellent support for the thermogenic activity of BAT.

Of note, alternative interpretations exist for some observations in this study. For example, the increase of whole-body EE in iBAPC-transplanted mice was relative to the mice that received mock transplantation or the mice themselves before the transplantation, wherein no adipocyte was present in muscle. Many adipokines (*e.g.*, leptin and adiponectin) have pivotal functions in whole-body energy homeostasis (53, 54). As such, the augmented EE in iBAPC-transplanted mice may not only be due to the thermogenesis of iBAPC grafts in muscle but also attributable to the paracrine and endocrine functions of the adipose grafts. In addition, although the swimming exercise in this study was done in warm water, we cannot exclude the possibility that the increase of *Ucp1* mRNA in long-term iBAPC grafts was due to cold exposure during swimming. Because both exercise and cold-exposure increase catecholamine levels, the effects of β-blocker propranolol did not favor either exercise or cold exposure as the cause of reversal of whitening in long-term iBAPC grafts. However, our data indeed indicated that iBAPC-derived adipose grafts in muscle, like BAT and beige fat in healthy people, can be activated in response to β-adrenergic activation, which further supports the potential of this transplantation strategy in future therapeutic applications.

It is also noteworthy that ectopic adipose tissue infiltration in muscle is commonly associated with disease conditions of skeletal muscles (*e.g.*, sarcopenia and muscular dystrophy) (55). Although the presence of intramuscular adipose engraftments did not alter the physical activity in this study, additional investigations are warranted to thoroughly examine the short-term and long-term impacts of intramuscular adipose grafts on muscle strength, performance, and metabolism.

The findings in this study also suggest a new way to bioengineer functional human BAT tissue *in vivo*. For example, future studies may explore the cotransplantation of human BAPCs with human vascular progenitor cells into skeletal muscles of immunodeficient large animal models (*e.g.*, SCID pigs) (56). With the aid of 3D matrix and scaffold biomaterials, such a strategy may provide sufficient human BAT implants for therapeutic applications in morbid obesity and patients with severe diabetes. FJ

ACKNOWLEDGMENTS

Research reported in this publication was supported by the National Institute of Arthritis and Musculoskeletal and Skin Diseases of the U.S. National Institutes of Health (NIH) under Award 1R01AR070178 and American Heart Association Grant-in-Aid 17GRNT33700260 to H.Y. The content is solely the responsibility of the authors and does not necessarily represent the official views of the NIH or American Heart Association. The authors declare no conflicts of interest.

AUTHOR CONTRIBUTIONS

Y. Liu and H. Yin designed the research; Y. Liu and W. Fu analyzed data; Y. Liu, W. Fu, K. Seese, and A. Yin performed the research; and Y. Liu and H. Yin wrote the manuscript.

REFERENCES

1. Cannon, B., and Nedergaard, J. (2004) Brown adipose tissue: function and physiological significance. *Physiol. Rev.* **84**, 277–359
2. Harms, M., and Seale, P. (2013) Brown and beige fat: development, function and therapeutic potential. *Nat. Med.* **19**, 1252–1263
3. Cypess, A. M., Lehman, S., Williams, G., Tal, I., Rodman, D., Goldfine, A. B., Kuo, F. C., Palmer, E. L., Tseng, Y. H., Doria, A., Kolodny, G. M., and Kahn, C. R. (2009) Identification and importance of brown adipose tissue in adult humans. *N. Engl. J. Med.* **360**, 1509–1517
4. Saito, M., Okamatsu-Ogura, Y., Matsushita, M., Watanabe, K., Yoneshiro, T., Nio-Kobayashi, J., Iwanaga, T., Miyagawa, M., Kameya, T., Nakada, K., Kawai, Y., and Tsujisaki, M. (2009) High incidence of metabolically active brown adipose tissue in healthy adult humans: effects of cold exposure and adiposity. *Diabetes* **58**, 1526–1531
5. Van Marken Lichtenbelt, W. D., Vanhommerig, J. W., Smulders, N. M., Drossaerts, J. M., Kemerink, G. J., Bouvy, N. D., Schrauwen, P., and Teule, G. J. (2009) Cold-activated brown adipose tissue in healthy men. *N. Engl. J. Med.* **360**, 1500–1508
6. Virtanen, K. A., Lidell, M. E., Orava, J., Heglind, M., Westergren, R., Niemi, T., Taittonen, M., Laine, J., Savisto, N. J., Enerbäck, S., and Nuutila, P. (2009) Functional brown adipose tissue in healthy adults. *N. Engl. J. Med.* **360**, 1518–1525

7. Zingaretti, M. C., Crosta, F., Vitali, A., Guerrieri, M., Frontini, A., Cannon, B., Nedergaard, J., and Cinti, S. (2009) The presence of UCP1 demonstrates that metabolically active adipose tissue in the neck of adult humans truly represents brown adipose tissue. *FASEB J.* **23**, 3113–3120
8. Wu, J., Boström, P., Sparks, L. M., Ye, L., Choi, J. H., Giang, A. H., Khandekar, M., Virtanen, K. A., Nuutila, P., Schaart, G., Huang, K., Tu, H., van Marken Lichtenbelt, W. D., Hoeks, J., Enerbäck, S., Schrauwen, P., and Spiegelman, B. M. (2012) Beige adipocytes are a distinct type of thermogenic fat cell in mouse and human. *Cell* **150**, 366–376
9. Sharp, L. Z., Shinoda, K., Ohno, H., Scheel, D. W., Tomoda, E., Ruiz, L., Hu, H., Wang, L., Pavlova, Z., Gilsanz, V., and Kajimura, S. (2012) Human BAT possesses molecular signatures that resemble beige/brite cells. *PLoS One* **7**, e49452
10. Carey, A. L., Formosa, M. F., Van Every, B., Bertovic, D., Eikelis, N., Lambert, G. W., Kalff, V., Duffy, S. J., Cherk, M. H., and Kingwell, B. A. (2013) Ephedrine activates brown adipose tissue in lean but not obese humans. *Diabetologia* **56**, 147–155
11. Orava, J., Nuutila, P., Noponen, T., Parkkola, R., Viljanen, T., Enerbäck, S., Rissanen, A., Pietiläinen, K. H., and Virtanen, K. A. (2013) Blunted metabolic responses to cold and insulin stimulation in brown adipose tissue of obese humans. *Obesity (Silver Spring)* **21**, 2279–2287
12. Dellagiacoma, G., Sbarbati, A., Rossi, M., Zancanaro, C., Benati, D., Merigo, F., Baldassarri, A., and Boicelli, A. (1992) Brown adipose tissue: magnetic resonance imaging and ultrastructural studies after transplantation in syngeneic rats. *Transplant. Proc.* **24**, 2986
13. Ferren, L. (1966) Morphological differentiation of implanted brown and white fats. *Trans. Kans. Acad. Sci.* **69**, 350–353
14. Gunawardana, S. C., and Piston, D. W. (2012) Reversal of type 1 diabetes in mice by brown adipose tissue transplant. *Diabetes* **61**, 674–682
15. Gunawardana, S. C., and Piston, D. W. (2015) Insulin-independent reversal of type 1 diabetes in nonobese diabetic mice with brown adipose tissue transplant. *Am. J. Physiol. Endocrinol. Metab.* **308**, E1043–E1055
16. Kikai, M., Yamada, H., Wakana, N., Terada, K., Yamamoto, K., Wada, N., Motoyama, S., Saburi, M., Sugimoto, T., Irie, D., Kato, T., Kawahito, H., Ogata, T., and Matoba, S. (2018) Adrenergic receptor-mediated activation of FGF-21-adiponectin axis exerts atheroprotective effects in brown adipose tissue-transplanted apoE$^{-/-}$ mice. *Biochem. Biophys. Res. Commun.* **497**, 1097–1103
17. Liu, X., Wang, S., You, Y., Meng, M., Zheng, Z., Dong, M., Lin, J., Zhao, Q., Zhang, C., Yuan, X., Hu, T., Liu, L., Huang, Y., Zhang, L., Wang, D., Zhan, J., Jong Lee, H., Speakman, J. R., and Jin, W. (2015) Brown adipose tissue transplantation reverses obesity in Ob/Ob mice. *Endocrinology* **156**, 2461–2469
18. Liu, X., Zheng, Z., Zhu, X., Meng, M., Li, L., Shen, Y., Chi, Q., Wang, D., Zhang, Z., Li, C., Li, Y., Xue, Y., Speakman, J. R., and Jin, W. (2013) Brown adipose tissue transplantation improves whole-body energy metabolism. *Cell Res.* **23**, 851–854
19. Nechad, M., and Olson, L. (1983) Development of interscapular brown adipose tissue in the hamster. II - differentiation of transplants in the anterior chamber of the eye: role of the sympathetic innervation. *Biol. Cell* **48**, 167–174
20. Stanford, K. I., Middelbeek, R. J., Townsend, K. L., An, D., Nygaard, E. B., Hitchcox, K. M., Markan, K. R., Nakano, K., Hirshman, M. F., Tseng, Y. H., and Goodyear, L. J. (2013) Brown adipose tissue regulates glucose homeostasis and insulin sensitivity. *J. Clin. Invest.* **123**, 215–223
21. Zhu, Z., Spicer, E. G., Gavini, C. K., Goudjo-Ako, A. J., Novak, C. M., and Shi, H. (2014) Enhanced sympathetic activity in mice with brown adipose tissue transplantation (transBATation). *Physiol. Behav.* **125**, 21–29
22. Ohno, H., Shinoda, K., Spiegelman, B. M., and Kajimura, S. (2012) PPARγ agonists induce a white-to-brown fat conversion through stabilization of PRDM16 protein. *Cell Metab.* **15**, 395–404
23. Boström, P., Mann, N., Wu, J., Quintero, P. A., Plovie, E. R., Panáková, D., Gupta, R. K., Xiao, C., MacRae, C. A., Rosenzweig, A., and Spiegelman, B. M. (2010) C/EBPβ controls exercise-induced cardiac growth and protects against pathological cardiac remodeling. *Cell* **143**, 1072–1083
24. Shamsi, F., and Tseng, Y. H. (2017) Protocols for generation of immortalized human brown and white preadipocyte cell lines. *Methods Mol. Biol.* **1566**, 77–85
25. Morrison, S., and McGee, S. L. (2015) 3T3-L1 adipocytes display phenotypic characteristics of multiple adipocyte lineages. *Adipocyte* **4**, 295–302
26. Tanis, R. M., Piroli, G. G., Day, S. D., and Frizzell, N. (2015) The effect of glucose concentration and sodium phenylbutyrate treatment on mitochondrial bioenergetics and ER stress in 3T3-L1 adipocytes. *Biochim. Biophys. Acta* **1853**, 213–221
27. Tran, T. T., and Kahn, C. R. (2010) Transplantation of adipose tissue and stem cells: role in metabolism and disease. *Nat. Rev. Endocrinol.* **6**, 195–213
28. Schulz, T. J., Huang, T. L., Tran, T. T., Zhang, H., Townsend, K. L., Shadrach, J. L., Cerletti, M., McDougall, L. E., Giorgadze, N., Tchkonia, T., Schrier, D., Falb, D., Kirkland, J. L., Wagers, A. J., and Tseng, Y. H. (2011) Identification of inducible brown adipocyte progenitors residing in skeletal muscle and white fat. *Proc. Natl. Acad. Sci. USA* **108**, 143–148
29. Ferrara, N. (2004) Vascular endothelial growth factor: basic science and clinical progress. *Endocr. Rev.* **25**, 581–611
30. Martin, B., Ji, S., Maudsley, S., and Mattson, M. P. (2010) "Control" laboratory rodents are metabolically morbid: why it matters. *Proc. Natl. Acad. Sci. USA* **107**, 6127–6133
31. Zouhal, H., Jacob, C., Delamarche, P., and Gratas-Delamarche, A. (2008) Catecholamines and the effects of exercise, training and gender. *Sports Med.* **38**, 401–423
32. Boström, P., Wu, J., Jedrychowski, M. P., Korde, A., Ye, L., Lo, J. C., Rasbach, K. A., Boström, E. A., Choi, J. H., Long, J. Z., Kajimura, S., Zingaretti, M. C., Vind, B. F., Tu, H., Cinti, S., Højlund, K., Gygi, S. P., and Spiegelman, B. M. (2012) A PGC1-α-dependent myokine that drives brown-fat-like development of white fat and thermogenesis. *Nature* **481**, 463–468
33. Lee, K. H., Nam, H., Jeong, E., Kim, S. S., Song, H. J., Pyeon, H. J., Kang, K., Hong, S. C., Nam, D. H., and Joo, K. M. (2016) Sensitive tumorigenic potential evaluation of adult human multipotent neural cells immortalized by hTERT gene transduction. *PLoS One* **11**, e0158639
34. Wilson, R., Urraca, N., Skobowiat, C., Hope, K. A., Miravalle, L., Chamberlin, R., Donaldson, M., Seagroves, T. N., and Reiter, L. T. (2015) Assessment of the tumorigenic potential of spontaneously immortalized and hTERT-immortalized cultured dental pulp stem cells. *Stem Cells Transl. Med.* **4**, 905–912
35. Tharp, K. M., Jha, A. K., Kraiczy, J., Yesian, A., Karateev, G., Sinisi, R., Dubikovskaya, E. A., Healy, K. E., and Stahl, A. (2015) Matrix-assisted transplantation of functional beige adipose tissue. *Diabetes* **64**, 3713–3724
36. Park, J., Kim, M., Sun, K., An, Y. A., Gu, X., and Scherer, P. E. (2017) VEGF-A-expressing adipose tissue shows rapid beiging and enhanced survival after transplantation and confers IL-4-independent metabolic improvements. *Diabetes* **66**, 1479–1490
37. Mahdaviani, K., Chess, D., Wu, Y., Shirihai, O., and Aprahamian, T. R. (2016) Autocrine effect of vascular endothelial growth factor-A is essential for mitochondrial function in brown adipocytes. *Metabolism* **65**, 26–35
38. Sun, K., Kusminski, C. M., Luby-Phelps, K., Spurgin, S. B., An, Y. A., Wang, Q. A., Holland, W. L., and Scherer, P. E. (2014) Brown adipose tissue derived VEGF-A modulates cold tolerance and energy expenditure. *Mol. Metab.* **3**, 474–483
39. Jo, D. H., Park, S. W., Cho, C. S., Powner, M. B., Kim, J. H., Fruttiger, M., and Kim, J. H. (2015) Intravitreally injected anti-VEGF antibody reduces brown fat in neonatal mice. *PLoS One* **10**, e0134308
40. Min, S. Y., Kady, J., Nam, M., Rojas-Rodriguez, R., Berkenwald, A., Kim, J. H., Noh, H. L., Kim, J. K., Cooper, M. P., Fitzgibbons, T., Brehm, M. A., and Corvera, S. (2016) Human 'brite/beige' adipocytes develop from capillary networks, and their implantation improves metabolic homeostasis in mice. *Nat. Med.* **22**, 312–318
41. Silva, F. J., Holt, D. J., Vargas, V., Yockman, J., Boudina, S., Atkinson, D., Grainger, D. W., Revelo, M. P., Sherman, W., Bull, D. A., and Patel, A. N. (2014) Metabolically active human brown adipose tissue derived stem cells. *Stem Cells* **32**, 572–581
42. Lee, C. W., Hsiao, W. T., and Lee, O. K. (2017) Mesenchymal stromal cell-based therapies reduce obesity and metabolic syndromes induced by a high-fat diet. *Transl. Res.* **182**, 61.e8–74.e8
43. Crisan, M., Casteilla, L., Lehr, L., Carmona, M., Paoloni-Giacobino, A., Yap, S., Sun, B., Léger, B., Logar, A., Pénicaud, L., Schrauwen, P., Cameron-Smith, D., Russell, A. P., Péault, B., and Giacobino, J. P. (2008) A reservoir of brown adipocyte progenitors in human skeletal muscle. *Stem Cells* **26**, 2425–2433
44. Kishida, T., Ejima, A., Yamamoto, K., Tanaka, S., Yamamoto, T., and Mazda, O. (2015) Reprogrammed functional brown adipocytes ameliorate insulin resistance and dyslipidemia in diet-induced obesity and type 2 diabetes. *Stem Cell Reports* **5**, 569–581

45. Hafner, A. L., Contet, J., Ravaud, C., Yao, X., Villageois, P., Suknuntha, K., Annab, K., Peraldi, P., Binetruy, B., Slukvin, I. I., Ladoux, A., and Dani, C. (2016) Brown-like adipose progenitors derived from human induced pluripotent stem cells: identification of critical pathways governing their adipogenic capacity. *Sci. Rep.* **6**, 32490
46. Ahfeldt, T., Schinzel, R. T., Lee, Y. K., Hendrickson, D., Kaplan, A., Lum, D. H., Camahort, R., Xia, F., Shay, J., Rhee, E. P., Clish, C. B., Deo, R. C., Shen, T., Lau, F. H., Cowley, A., Mowrer, G., Al-Siddiqi, H., Nahrendorf, M., Musunuru, K., Gerszten, R. E., Rinn, J. L., and Cowan, C. A. (2012) Programming human pluripotent stem cells into white and brown adipocytes. *Nat. Cell Biol.* **14**, 209–219
47. Bowman, W. C., and Nott, M. W. (1969) Actions of sympathomimetic amines and their antagonists on skeletal muscle. *Pharmacol. Rev.* **21**, 27–72
48. Altshuler-Keylin, S., Shinoda, K., Hasegawa, Y., Ikeda, K., Hong, H., Kang, Q., Yang, Y., Perera, R. M., Debnath, J., and Kajimura, S. (2016) Beige adipocyte maintenance is regulated by autophagy-induced mitochondrial clearance. *Cell Metab.* **24**, 402–419
49. Bartness, T. J., Vaughan, C. H., and Song, C. K. (2010) Sympathetic and sensory innervation of brown adipose tissue. *Int. J. Obes.* **34** (Suppl 1), S36–S42
50. Roh, H. C., Tsai, L. T. Y., Shao, M., Tenen, D., Shen, Y., Kumari, M., Lyubetskaya, A., Jacobs, C., Dawes, B., Gupta, R. K., and Rosen, E. D. (2018) Warming induces significant reprogramming of beige, but not brown, adipocyte cellular identity. *Cell Metab.* **27**, 1121.e5–1137.e5
51. Almind, K., Manieri, M., Sivitz, W. I., Cinti, S., and Kahn, C. R. (2007) Ectopic brown adipose tissue in muscle provides a mechanism for differences in risk of metabolic syndrome in mice. *Proc. Natl. Acad. Sci. USA* **104**, 2366–2371
52. Yin, H., Pasut, A., Soleimani, V. D., Bentzinger, C. F., Antoun, G., Thorn, S., Seale, P., Fernando, P., van Ijcken, W., Grosveld, F., Dekemp, R. A., Boushel, R., Harper, M. E., and Rudnicki, M. A. (2013) MicroRNA-133 controls brown adipose determination in skeletal muscle satellite cells by targeting Prdm16. *Cell Metab.* **17**, 210–224
53. Ahima, R. S., and Flier, J. S. (2000) Leptin. *Annu. Rev. Physiol.* **62**, 413–437
54. Chandran, M., Phillips, S. A., Ciaraldi, T., and Henry, R. R. (2003) Adiponectin: more than just another fat cell hormone? *Diabetes Care* **26**, 2442–2450
55. Hausman, G. J., Basu, U., Du, M., Fernyhough-Culver, M., and Dodson, M. V. (2014) Intermuscular and intramuscular adipose tissues: bad vs. good adipose tissues. *Adipocyte* **3**, 242–255
56. Suzuki, S., Iwamoto, M., Saito, Y., Fuchimoto, D., Sembon, S., Suzuki, M., Mikawa, S., Hashimoto, M., Aoki, Y., Najima, Y., Takagi, S., Suzuki, N., Suzuki, E., Kubo, M., Mimuro, J., Kashiwakura, Y., Madoiwa, S., Sakata, Y., Perry, A. C. F., Ishikawa, F., and Onishi, A. (2012) Il2rg gene-targeted severe combined immunodeficiency pigs. *Cell Stem Cell* **10**, 753–758

Received for publication October 9, 2018.
Accepted for publication April 8, 2019.